ELSEVIER

Polymer 41 (2000) 8355–8362

polymer

www.elsevier.nl/locate/polymer

The biphasic behaviour of a thermotropic polymesomorphic polyester
I. Time evolution of phase separation

M.C. Righetti[a,*], M. Laus[b]

[a]Centro di Studio per la Fisica delle Macromolecole-CNR, Via Selmi 2, 40126 Bologna, Italy
[b]Dipartimento di Scienze e Tecnologie Avanzate-Università del Piemonte Orientale 'A.Avogadro', Corso Borsalino 54, 15100 Alessandria, Italy

Received 6 March 2000; accepted 21 March 2000

Abstract

The time evolution of biphase segregation at the nematic–isotropic (N–I) as well as the S_a–N and S_b–S_a transitions of a main chain polyester was studied by annealing the sample inside the relevant biphasic regions. Only the splitting of the N–I transition process is observed when the sample is annealed at a temperature in the N–I biphasic gap. In contrast, when the sample is annealed at a temperature in the biphasic regions involving a smectic phase, both the S_a–N and S_b–S_a processes are split into two components, whereas the N–I transition process is found to be little affected by the thermal treatment. The peak temperature difference between the biphase segregated components and the overall peak resolution indicates that the more efficient segregation occurs for the transition at which the biphasic separation had been performed.

The overall phenomenology shows that the molar mass distribution in the two biphase segregated components is: (a) optimized for the specific transition at which the biphasic separation is performed; and (b) different for the various transitions according to their distinct symmetry and steric packing features. © 2000 Published by Elsevier Science Ltd.

Keywords: Thermotropic polyester; Thermal characterization; Biphasic segregation

1. Introduction

The thermodynamic and kinetic aspects of the isotropic–anisotropic biphasic equilibria in thermotropic liquid crystalline polymeric systems are under investigation from both theoretical and experimental points of view [1–16]. On account of the equilibrium nature of the liquid crystalline transitions, the biphasic behaviour of these polymeric systems can be easily outlined under conditions approaching thermodynamic equilibrium. Accordingly, new aspects of the segregation phenomena can be highlighted, improving the knowledge of the thermodynamics of semiflexible chain molecules. In addition, by a careful control of the thermal history of the samples, it should be possible to obtain materials with predetermined microsegregated morphologies and unconventional physico-chemical properties.

The occurrence of a thermodynamically stable biphasic region located between the pure nematic phase and the pure isotropic phase has been described in semiflexible main chain copolymers with statistical distribution of rigid and flexible segments along the chain backbone [1–5]. The statistical fluctuations in the chain composition of these copolymers are supposed to produce a distribution of flexibilities, called polyflexibility, capable of promoting partitioning between the nematic and isotropic liquid phases that coexist over a very wide range of temperatures. A substantial incorporation of the more rigid chains into the nematic mesophase is expected. Theoretical calculations are in agreement with the above explanation of the biphasic behaviour of liquid crystalline statistical copolymers [6,7].

In contrast, the nematic–isotropic (N–I) biphasic behaviour of main chain polymers with regular structure is primarily ascribed to the molar mass characteristics of the samples [8–13]. In fact, in order to observe an N–I biphase separation, the average molar mass of the sample should be fairly high and the mass distribution quite wide [13], so that the phase transition parameters of the individual species could differ substantially, according to their distinct molar mass dependencies. A hypothesis was formulated [13], according to which the N–I biphase segregation in main chain polymers with regular structure should be mainly driven by a screening mechanism of entropic origin, in which the lower molar mass species segregate from the longer chain molecules. As the two segregated components

---

* Corresponding author. Fax: +39-051-2099456.
E-mail address: righetti@ciam.unibo.it (M.C. Righetti).

PII: S0032-3861(00)00249-4

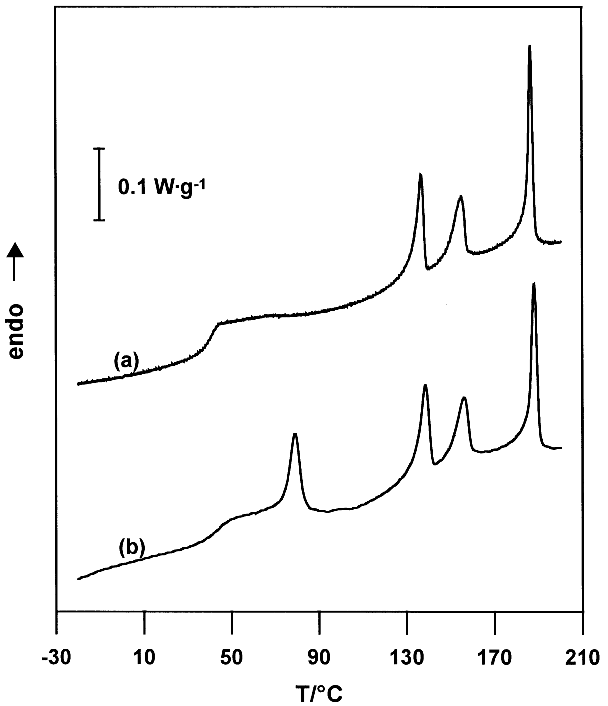

Fig. 1. DSC heating curves (10°C/min) for polymer **I**: (a) after rapid cooling from the isotropic phase; and (b) after thermal treatment at 60°C for 24 h.

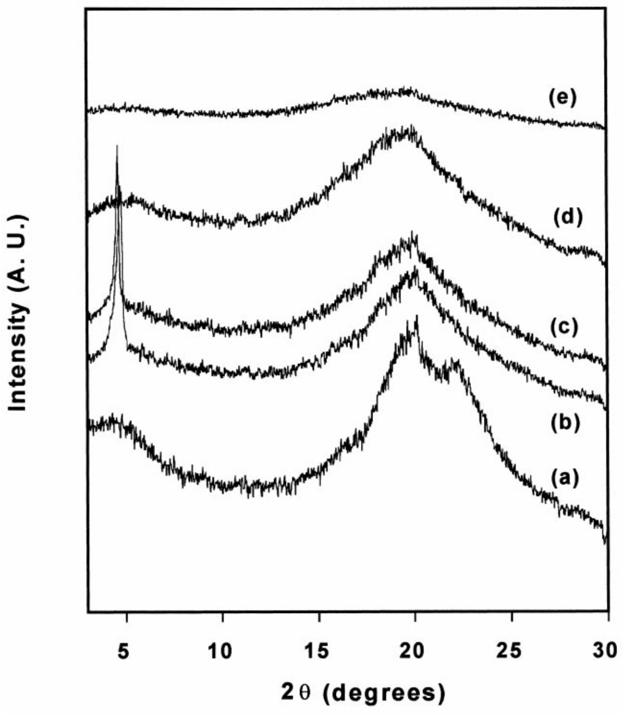

Fig. 2. X-ray spectra for polymer **I** at: (a) room temperature; (b) 100°C; (c) 145°C; (d) 180°C; and (e) 210°C.

present substantially different average molar mass values, two distinct N–I transitions are observed in the corresponding differential scanning calorimetry (DSC) thermograms, the endotherms at lower and higher temperatures being associated with the fractions with lower and higher molar mass, respectively.

Polymers presenting smectic and nematic mesophases are of special interest for the present investigation because the comparison between the biphasic behaviour at the N–I as well as at the smectic–nematic or smectic–smectic transitions should allow the driving force towards microphase segregation to be understood better, and the structural and molecular factors conducive to separation in the various LC phases, differing in their stability and degree of order, to be delineated.

Accordingly, in the present study we describe the time evolution of biphase segregation at the N–I as well as the S_a–N and S_b–S_a transitions of a main chain polymer with the following structure:

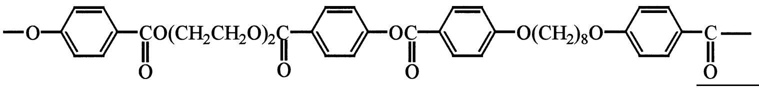

$$-O-C_6H_4-\underset{\overset{\|}{O}}{C}O(CH_2CH_2O)_2\underset{\overset{\|}{O}}{C}-C_6H_4-O\underset{\overset{\|}{O}}{C}-C_6H_4-O(CH_2)_8O-C_6H_4-\underset{\overset{\|}{O}}{C}-$$

which presents three LC mesophases, namely a nematic, a smectic A and a smectic B phase. In a forthcoming paper [17], the entire biphase segregation phenomenology will be reported as a function of the annealing temperature.

2. Experimental

Polymer **I** was prepared by a condensation reaction under phase transfer conditions, according to the procedure previously reported [18], and purified by precipitations from chloroform solution into methanol. The number average molar mass M_n and the first polydispersity index M_w/M_n are 18 000 and 2.1, respectively.

DSC analyses were carried out using a Perkin–Elmer DSC 7 apparatus. Samples of about 5 mg were employed. The instrument was calibrated in temperature and energy with high purity standards (indium, naphthalene, benzoic acid, cyclohexane) at 10°C min^{-1}. Dry nitrogen was used as purge gas. A preliminary characterization of polymer **I** was performed in the temperature range between −30 and 200°C. Afterwards, the time evolution of biphasic segregation was studied according to the following procedure. Polymer **I** samples were heated up to 200°C and kept at this temperature for 20 min in order to cancel the previous thermal history. Subsequently, they were cooled at a nominal rate of 200°C min^{-1} to a selected temperature T_a, chosen in the region associated with the mesophase transitions. After annealing at this temperature for various times,

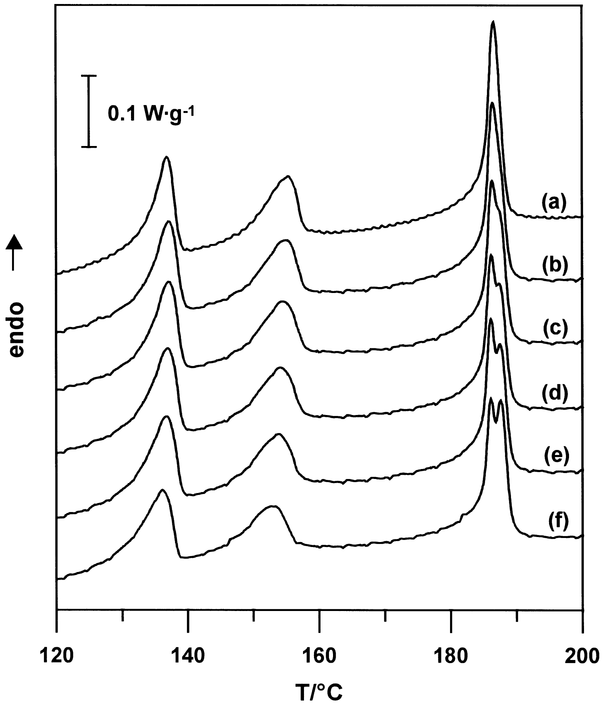

Fig. 3. DSC heating curves (10°C/min) for polymer **I** after annealing at $T_a = 185.3$°C and successive cooling to 50°C (annealing times: (b) 1 h; (c) 3 h; (d) 5 h; (e) 8 h; and (f) 23.5 h). Curve (a) is obtained after rapid cooling from the isotropic phase.

the samples were cooled to 50°C or to a temperature immediately before the beginning of the transition. The samples were finally subjected to a heating run up to 200°C at a rate of 10°C min^{-1} and the corresponding DSC curves collected and analysed.

The above annealing treatment did not produce appreciable chain degradation or structural scrambling. The transition temperatures were determined as the peak values of the endothermic processes, the glass transition was taken as the fictive temperature [19].

3. Results and discussion

Fig. 1 reports the DSC heating curves of polymer **I** after rapid cooling from the isotropic phase (trace a) and after thermal treatment at 60°C for 24 h (trace b). In the first case, a well-defined step due to the glass transition is observed at 36°C ($\Delta c_p = 195\ J\ mol^{-1}\ K^{-1}$), followed by three sharp endothermic transitions at 137°C ($\Delta S = 6.8\ J\ mol^{-1}\ K^{-1}$), 155°C ($\Delta S = 5.7\ J\ mol^{-1}\ K^{-1}$), and 187°C ($\Delta S = 8.6\ J\ mol^{-1}\ K^{-1}$), respectively. In the DSC trace of the sample annealed at 60°C, an additional transition centred at 79°C is observed. Combined thermal optical analysis (TOA) and X-ray diffraction analysis (Fig. 2) showed that the three endothermic peaks at the higher temperatures are associated with S_b–S_a, S_a–N and N–I transitions, respectively, and that the endothermic process observed in the annealed sample corresponds to the melting.

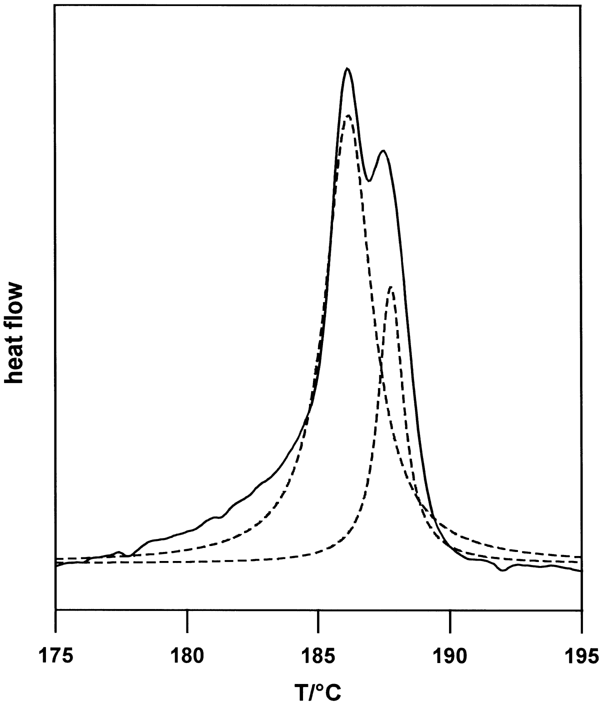

Fig. 4. Example of the non-linear fitting for the DSC curve portion associated with the N–I transition: (solid line) experimental curve; and (dashed lines) resolved curves.

The biphasic behaviour and the kinetics of phase segregation of polymer **I** was delineated for each mesomorphic transition by DSC according to the procedure described in Section 2.

For each biphasic region, the annealing temperature T_a was chosen in order to observe, after a sufficiently long time, the splitting of the original endothermic peak into two well-resolved components of comparable intensity. As reported in detail in a forthcoming paper [17], the DSC endothermic associated with the N–I, S_a–N and S_b–S_a transitions fulfil this condition when the annealing temperatures are 185.3, 153 and 135.6°C, respectively. The time evolution of the biphasic segregation processes at these temperatures is described separately in the following sections for the three different mesomorphic transitions.

3.1. Biphasic segregation at the N–I transition

Fig. 3 illustrates some DSC heating curves after different annealing times at 185.3°C (inside the N–I biphasic region) and fast cooling down to 50°C. The N–I peak is split into components that emerge progressively better resolved with increasing time. On the contrary, the endothermic peaks associated with the S_b–S_a and S_a–N transitions do not appear to be affected by the above thermal treatment.

In order to separate the two overlapping peaks in the N–I region, a non-linear curve fitting was performed with multiple Lorentzian peaks. Fig. 4 reports an example of

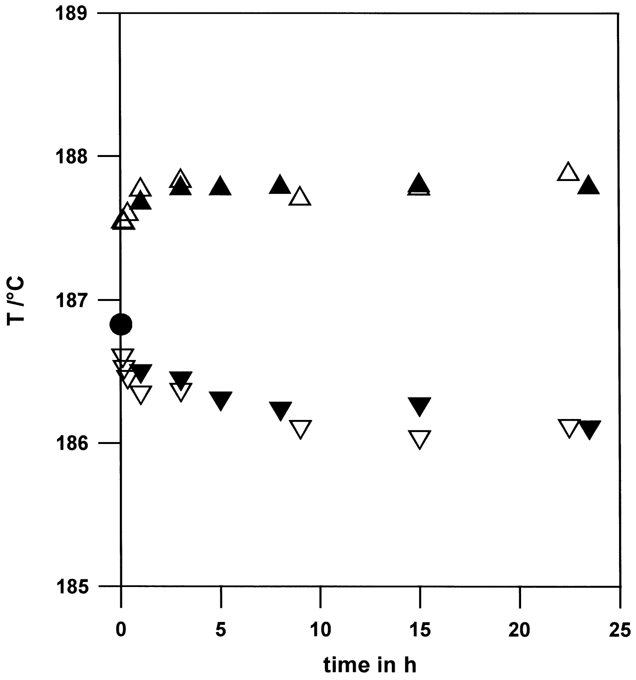

Fig. 5. Temperatures of the two resolved N–I transition peaks as a function of the annealing time at $T_a = 185.3°C$: (▼) and (▲) after cooling to 50°C; (▽) and (△) after cooling to 170°C (see text). The temperature of the non-annealed peak is also shown (●).

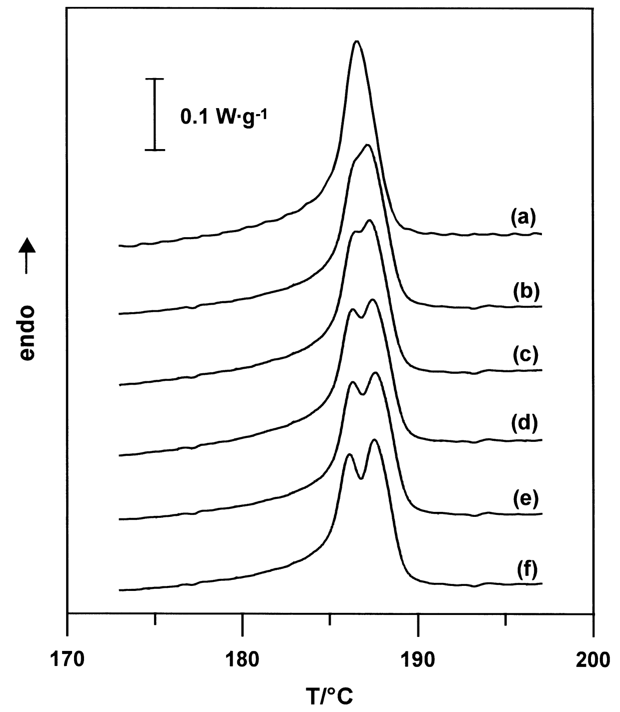

Fig. 7. DSC heating curves (10°C/min) for polymer **I** after annealing at $T_a = 185.3°C$ and successive cooling to 170°C (annealing times: (b) 10 min; (c) 20 min; (d) 30 min; (e) 3 h; and (f) 22.5 h). Curve (a) is obtained after rapid cooling from the isotropic phase.

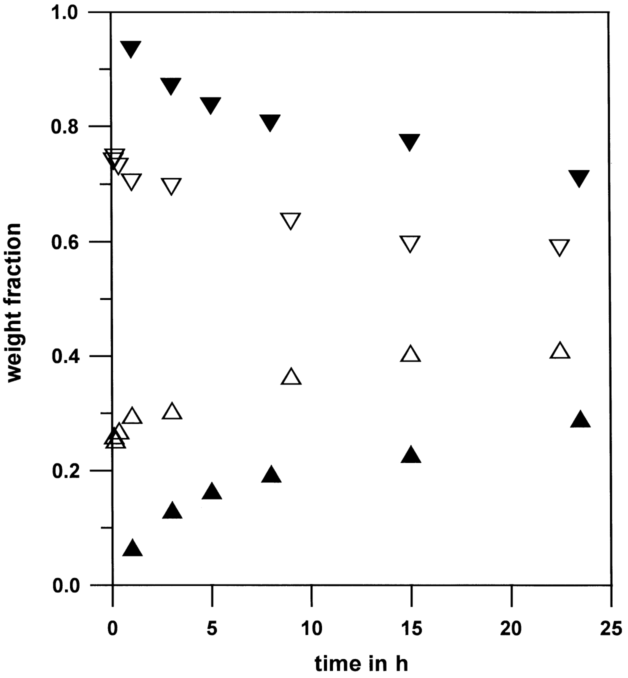

Fig. 6. Weight fraction of the two resolved N–I transition components as a function of the annealing time at $T_a = 185.3°C$: low-temperature peak (▼) and high-temperature peak (▲) after cooling to 50°C; low-temperature peak (▽) and high-temperature peak (△) after cooling to 170°C (see text).

the performed fit. The sum of the two resolved endotherms does not reproduce perfectly the experimental curve in the low- and high-temperature sides of the N–I endotherm. Nevertheless, the error introduced in the determination of the relative percentage of the two components is estimated less than 10%. Moreover, it has to be noted that the area of the low-temperature component is always found by the fitting procedure higher than that of the high-temperature component because of the broadening that is observed in the low-temperature side of the N–I transition.

Fig. 5 shows the temperatures of the two resolved N–I transition peaks as a function of the annealing time. The two components are observed at temperatures higher and lower with respect to the temperature of the non-annealed peak. The relative percentages, obtained from the two resolved areas, are reported in Fig. 6 as a function of time. The fractional area of the high-temperature peak increases with time and tends to a limiting value whereas the mirroring trend is obviously observed for the low-temperature peak. This behaviour suggests that the separation process produces a multidomain structure, initially characterized by few and/or small domains comprising high molar mass species. The size and/or the number of these domains progressively increase with increasing the annealing time at T_a.

In order to verify if remixing of the two nematic fractions could occur during cooling to 50°C, the following experiment was performed. After annealing at T_a, the samples

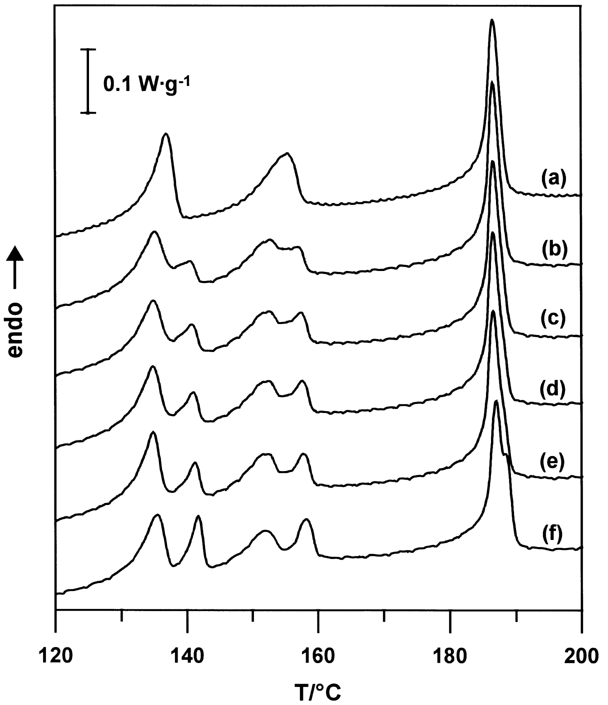

Fig. 8. DSC heating curves (10°C/min) for polymer **I** after annealing at $T_a = 153$°C and successive cooling to 50°C (annealing times: (b) 10 min; (c) 30 min; (d) 1 h; (e) 3 h; and (f) 22 h). Curve (a) is obtained after rapid cooling from the isotropic phase.

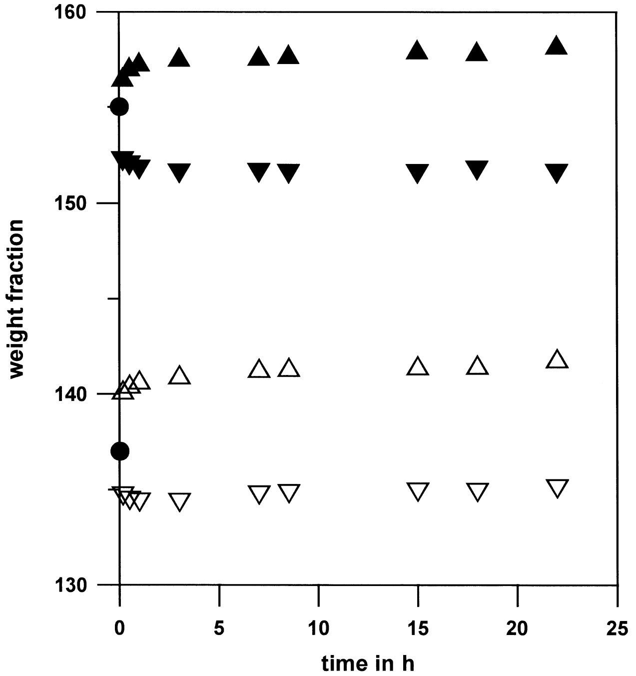

Fig. 9. Temperatures of the resolved S_b–S_a (▽ and △) and S_a–N (▼ and ▲) transition peaks as a function of the annealing time at $T_a = 153$°C. The temperatures of the non-annealed peaks are also shown (●).

were fast cooled to 170°C, a temperature before the beginning of the transition, and promptly reheated. The corresponding DSC heating curves are shown in Fig. 7 and the resolved N–I transition temperatures and areas in Figs. 5 and 6, respectively. The peak temperatures after cooling to 170°C and immediate reheating are practically coincident with those obtained after cooling to 50°C (Fig. 5), but from Fig. 6 it is evident that a more efficient separation is observed after cooling to 170°C. It turns out that remixing of the separated polymeric fractions occurs to a little extent during the cooling and the heating steps of the experiments illustrated in Fig. 3. In addition, it is worth noting that the enthalpy associated with the N–I endotherm after the biphasic segregation is equal to that of the original non-annealed peak.

3.2. Biphasic segregation at the S_a–N transition

Fig. 8 illustrates some DSC heating curves from 50°C after various annealing times in the S_a–N biphasic region at $T_a = 153.0$°C. After about 10 min of annealing, the S_a–N peak begins to split into two components. Under these conditions also the S_b–S_a transition process appears structured into two well-resolved components whose time evolution parallels that of the S_a–N transition. In contrast, the N–I process seems little affected by the thermal treatment. Only after a treatment longer than 15 h, a shoulder in the high-temperature peak region can be observed.

The DSC curves obtained after cooling to temperatures immediately before the beginning of the transitions were found not to change, indicating that mixing of the separated fractions does not occur during cooling to 50°C. On the contrary, mixing of the two separated fractions occurs at temperatures higher than 160°C, as evidenced by the following experiment. After annealing at 153°C for different times, samples were analysed from 50 to 180°C, rapidly cooled to 50°C, and finally reheated. After this thermal treatment, the DSC curves showed endotherms coincident with those of the non-annealed sample.

Using the fitting procedure above described, the peak temperatures and the relative percentage of the two components were evaluated for the S_a–N and S_b–S_a transition processes after annealing in the S_a–N biphasic regions. The results are shown in Figs. 9 and 10, respectively. Also in this case the components of both S_a–N and S_b–S_a transitions are observed at temperatures higher and lower than the original peaks (Fig. 9). In addition, for both transitions, the fractional areas of the low- and high-temperature peaks of both transitions decrease and increase with time, respectively, and tend to be limiting values. After approximately 20 h of annealing (Fig. 10), the process can be considered accomplished.

As far as the enthalpy change is concerned, it is interesting to note that the enthalpy associated with the S_b–S_a and the N–I transitions after the biphasic separation is equal to that measured for the relevant non-annealed peaks. In contrast, the enthalpy change for the S_a–N transition is

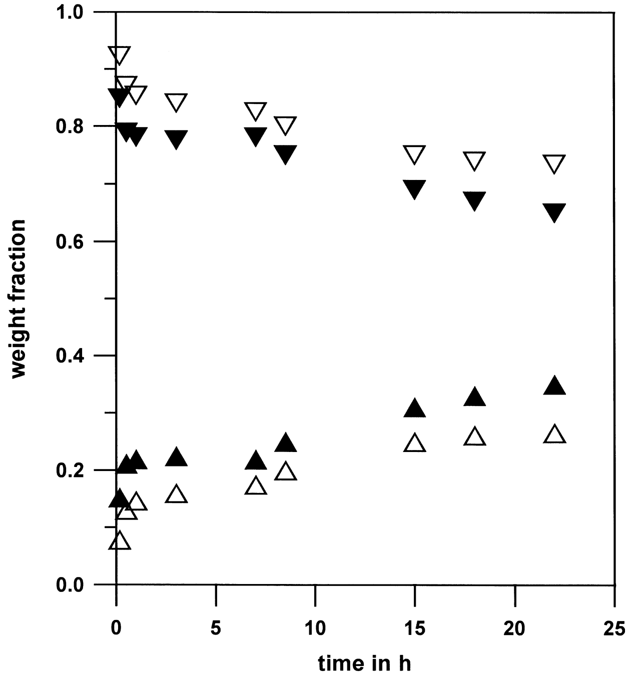

Fig. 10. Weight fraction of the resolved S_b–S_a (▽ and △) and S_a–N (▼ and ▲) transition components as a function of the annealing time at $T_a = 153°C$: low-temperature peak (▽ and ▼) and high-temperature peak (△ and ▲).

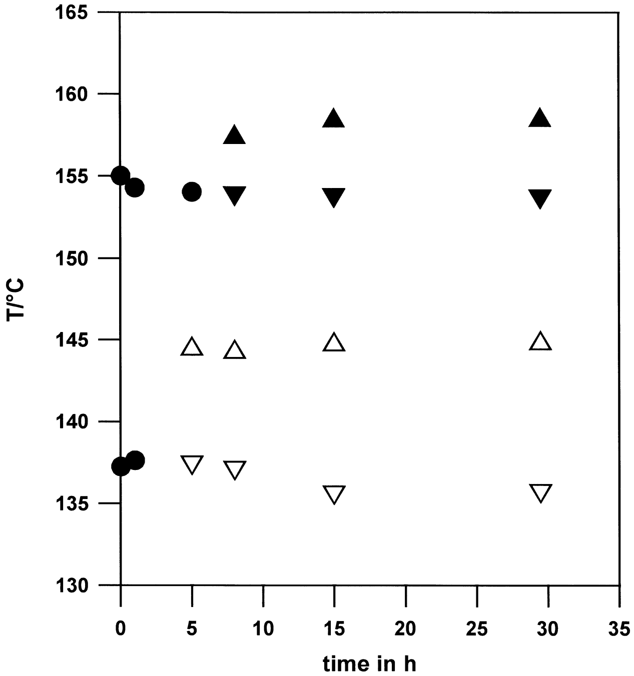

Fig. 12. Temperatures of the resolved S_b–S_a (▽ and △) and S_a–N (▼ and ▲) transition peaks as a function of the annealing time at $T_a = 135.6°C$. The temperatures of the non-annealed and non-split peaks are also shown (●).

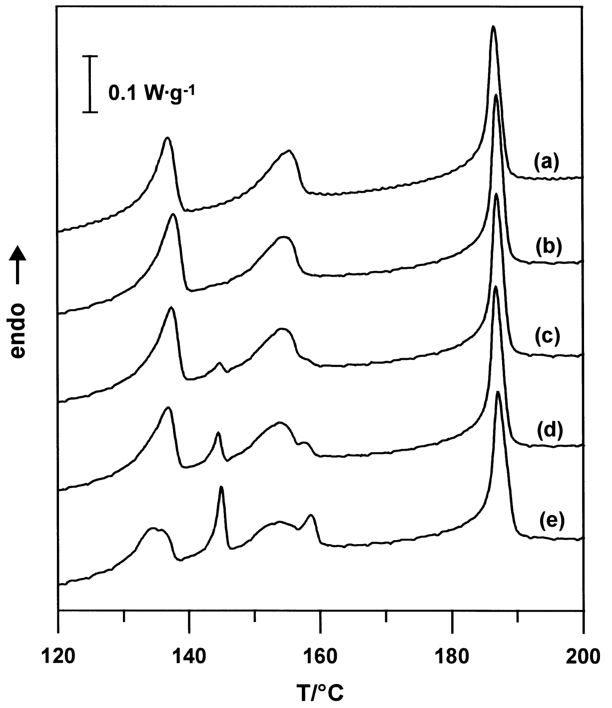

Fig. 11. DSC heating curves (10°C/min) for polymer **I** after annealing at $T_a = 135.6°C$ and successive cooling to 50°C (annealing times: (b) 1 h; (c) 5 h; (d) 8 h; and (e) 29.5 h). Curve (a) is obtained after rapid cooling from the isotropic phase.

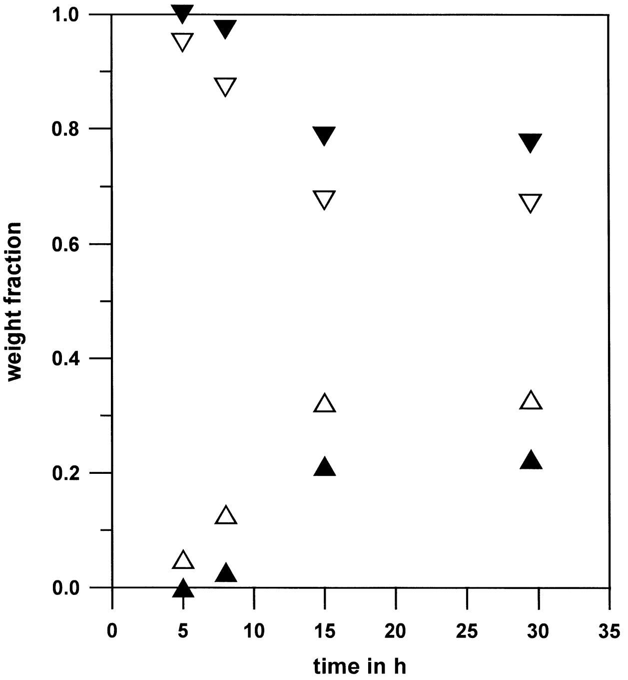

Fig. 13. Weight fraction of the resolved S_b–S_a (▽ and △) and S_a–N (▼ and ▲) transition components as a function of the annealing time at $T_a = 135.6°C$: low-temperature peak (▽ and ▼) and high-temperature peak (△ and ▲).

found to be appreciably lower (10%) than that of the original peak.

3.3. Biphasic segregation at the S_b–S_a transition

Fig. 11 shows some DSC heating curves after various annealing times at 135.6°C, in the S_b–S_a biphasic region. In this case, the time evolution of the biphasic separation process is different from that observed at the S_a–N and N–I transitions. After 1 h of annealing the DSC trace does not change, thus indicating the existence of an apparent induction period probably due to the fact that the diffusion rate of the polymeric chains is low at this temperature. Only after 5 h, a low-intensity peak emerges from the background in the high-temperature side of the S_b–S_a transition and increases in intensity without changing its temperature position. The time evolution of the S_a–N process closely parallels that of the S_b–S_a process, showing a peak whose intensity increases progressively with time. The shape of the DSC peak associated to the N–I transition is unaffected by the thermal treatment in the S_b–S_a biphasic region.

Figs. 12 and 13 illustrate the peak temperatures and the relative percentage of the S_b–S_a and S_a–N components segregated in the S_b–S_a biphasic region. An induction time of about 5 h for the segregation process is well evident for both S_b–S_a and S_a–N transitions. Moreover, for both the transitions the temperature of the low-temperature peak is approximately equal to that of the original non-annealed peak, in contrast to the high-temperature peak, which is found, especially for the S_b–S_a transition, at temperatures remarkably higher.

Also in this case, a reduction of the enthalpy change is observed for the S_a–N transition after the annealing treatment with respect to the untreated sample, whereas the enthalpy changes associated to the S_b–S_a and the N–I transitions are constant.

4. Conclusions

The time evolution of biphase segregation at the N–I as well as S_a–N and S_b–S_a transitions of a main chain polyester was studied by annealing the sample inside the relevant biphasic gaps. Although the overall phenomenology of the biphasic behaviour of this polymesomorphic polymer is quite complex, there are some features that deserve particular interest. When the sample is annealed at a temperature in the N–I biphasic region, the only observed splitting is associated with the N–I transition process. The S_b–S_a and S_a–N processes are not affected by the demixing that occurred during the annealing in the N–I biphasic region. This indicates that the smectic mesophases are insensitive to the molar mass features that produce two distinct N–I transitions. On the contrary, when the sample is annealed at a temperature in the biphasic regions involving a smectic phase, both the S_a–N and S_b–S_a processes appear separated into two components, whereas the N–I transition process is found little affected by the thermal treatment. This phenomenology suggests that the molar mass characteristic of the biphasic separated fractions are completely different for the various mesophases, in agreement with their distinct degree of order.

The peak temperature difference between the biphase segregated components and the peak separation are comparatively greater for the transition at which the biphasic separation is performed, thus indicating that the more efficient segregation occurs for the transition at which the biphasic separation is carried out.

As far as the enthalpy change is concerned, the finding that the enthalpy absorbed during the passage from the separated S_a phases to the nematic phase is lower than that absorbed by a non-segregated sample indicates that the energy necessary to modify the S_a segregated structure is lower and suggests that the interaction forces in the segregated structure are less strong.

The overall phenomenology described in this paper shows that the segregation of molecules with different molar mass is optimized for the specific transition at which the biphasic separation is performed and is different for the various transitions. This clearly indicates that the steric packing features specific for the various mesophases at equilibrium at their biphasic temperature are able to select and incorporate specific molar masses that are more compliant with the symmetry and chain organization dictated by the liquid crystalline order.

Acknowledgements

Financial support from Ministero dell'Università e della Ricerca Scientifica e Tecnologica of Italy is acknowledged.

References

[1] Moore SJ, Stupp SI. Macromolecules 1987;20:273.
[2] Moore SJ, Stupp SI. Macromolecules 1987;20:282.
[3] Moore SJ, Stupp SI. Macromolecules 1988;21:1217.
[4] Martin PG, Stupp SI. Macromolecules 1988;21:1222.
[5] Stupp SI, Moore JS, Martin PG. Macromolecules 1988;21:1228.
[6] Fredrickson GH. Macromolecules 1989;22:2746.
[7] Fredrickson GH, Leibler L. Macromolecules 1990;23:531.
[8] D'Allest JF, Wu PP, Blumstein A, Blumstein RB. Mol Cryst Liq Cryst Lett 1986;3:103.
[9] D' Allest JF, Sixou P, Blumstein A, Blumstein RB. Mol Cryst Liq Cryst 1988;157:229.
[10] Kim DJ, D' Allest JF, Blumstein A, Blumstein RB. Mol Cryst Liq Cryst 1988;157:253.
[11] Laus M, Caretti D, Angeloni AS, Galli G, Chiellini E. Macromolecules 1991;24:1459.
[12] Chiellini E, Galli G, Laus M, Angeloni AS, Caretti D. Mol Cryst Liq Cryst 1991;215:101.
[13] Laus M, Angeloni AS, Galli G, Chiellini E. Macromolecules 1992;25:5901.

[14] Viney C, Yoon DY, Beck B, Ringsdorf H. Macromolecules 1991;22:4088.

[15] Ratto JA, Volino F, Blumstein RB. Macromolecules 1991;24:2862.

[16] Galli G, Chiellini E, Laus M, Caretti D, Angeloni AS. Makromol Chem Rapid Commun 1991;12:43.

[17] Righetti MC, Laus M. In preparation.

[18] Galli G, Chiellini E, Angeloni AS, Bignozzi MC. J Mater Chem 1994;4:429.

[19] Richardson MJ. In: Allen G, Bevington JC, editors. Thermal analysis, Comprehensive polymer science, Vol. 1. Oxford: Pergamon Press, 1989. p. 867–901.